Weldability of Nitrogen-Strengthened Stainless Steels

The addition of nitrogen increases yield strength at subzero temperatures and improves resistance to attack by pitting type corrosive media

BY R. H. ESPY

ABSTRACT. The development of the nitrogen-strengthened austenitic stainless steels has resulted in materials having interesting and useful properties that are quite different from the conventional AISI 300 series of stainless steels. The element nitrogen performs several very interesting functions. Nitrogen not only strengthens the steel at room temperature, but its addition imparts the property of increasing yield strength at subzero temperatures.

In pitting type corrosive media, nitrogen (like molybdenum and chromium) improves resistance to attack. Where nitrogen alloying permits, the use of nickel content less than 6% or silicon additions improves resistance to transgranular stress corrosion cracking. Nitrogen added to the steel inhibits carbon migration so that weld areas show little carbide precipitation even at 0.06% carbon. These attractive features of nitrogen additions are used in four commercial alloys, each designed to maximize properties of special interest.

Weld filler deposits for four base metal compositions required composition adjustments to achieve structures of ferrite in a matrix of austenite. Nitrogen content was also lowered to minimize occurrence of porosity. The nitrogen levels employed with the two phase structures were generally sufficient to give weldment tensile strengths equal to those of the unwelded base metals. In autogenous welding, special practices like reduced travel speeds or refusion techniques are required to avoid porosity associated with the high base metal nitrogen content.

Introduction

The development of the nitrogen strengthened austenitic stainless steels has resulted in materials having interesting and useful properties that are quite different from the conventional AISI 300 series of stainless steels. Nitrogen performs several functions. It not only strengthens at room temperature but the nitrogen addition imparts the property of increasing yield strengths at sub zero temperatures. Surface hardening by metal and particle abrasion results in unusually good wear and galling characteristics.

In pitting type corrosion media, nitrogen, like molybdenum and chromium, improves resistance to attack. Where nitrogen alloying permits, the use of nickel contents less than 6% or silicon additions improved resistance to transgranular stress corrosion cracking. Nitrogen additions inhibit carbon migration so that weld heat-affected zones show little carbide precipitation even at 0.06% carbon, and show reduced carbide precipitation at carbon levels above 0.06%.

These properties are used by Armco in its NITRONIC* stainless steel nos. 33, 40, 50 and 60—each designed to optimize properties of special interest. To better understand the effect of nitrogen alloying in austenite, information on the four alloys is presented. Composition, mechanical properties, cold work hardening, wear and galling, corrosion resistance and weldability are covered. In each case, Type 304 stainless is included for comparison.

Composition

Alloys 33, 40, 50 and 60 are chemically balanced to have an austenite stability well above that of Type 304 stainless. The compositions are shown in Table 1. The four alloys are available in most product forms with the exception of alloy 60 which has not been available in sheet form.

Mechanical Properties

The effect of nitrogen as a solid solution strengthener is very evident on mechanical properties as shown in Tables 2, 3 and 4. Yield strengths at room temperature are about 20 ksi (138 MPa) higher than that of Type 304, and ultimate tensile strengths also average about 20 ksi (138 MPa) higher.

At temperatures below room temperature, solid solution strengtheners have

**NITRONIC is a trademark of Armco Inc., Middletown, Ohio.*

Table 1—Typical Compositions of NITRONIC Stainless Steel Alloys

Alloy type	C	Mn	Si	Cr	Ni	Mo	N	V	Cb	Austenite[a] stability factor
33	.05	12.5	.40	17.50	3.5	–	.31	–	–	44.30
40	.03	9.0	.60	20.50	6.7	–	.30	–	–	46.40
50	.04	5.0	.40	21.25	12.2	2.2	.27	.15	.15	49.95
60	.07	8.0	4.00	16.50	8.2	–	.14	–	–	39.00
AISI 304	.06	1.4	.50	18.25	9.0	–	.04	–	–	30.65

(a) (30 × %C) + %Mn + %Cr + %Ni + %Mo + (30 × %N) = Austenite stability factor

Based on paper sponsored by the American Iron and Steel Institute for presentation at the AWS 61st Annual Meeting held in Los Angeles, California, during April 14-18, 1980.

R. H. ESPY, now retired, was with Armco Inc., Middletown, Ohio, at the time of the paper's presentation at the AWS 61st Annual Meeting.

Table 2—Mechanical Properties[a] of Alloys 33, 40, 50 and 60 at Room Temperature

Alloy	UTS, ksi (MPa)	0.2%YS, ksi (MPa)	El, %	RA, %	CVN, ft-lb (J)
33	110 (758)	60 (414)	55	70	230 (313)
40	110 (690)	57 (393)	53	75	205 (279)
50	120 (827)	60 (414)	50	70	170 (231)
60	103 (710)	60 (414)	64	74	> 240 (> 326)
AISI 304	86 (593)	40 (276)	60	70	185 (252)

(a) UTS—ultimate tensile strength; YS—yield strength; El—elongation in 2 in. (50.8 mm); RA—reduction in area; CVN—Charpy V-notch.

Table 3—Mechanical Properties[a] of Alloys 33, 40, 50 and 60 at −320°F (−196°C)

Alloy	UTS, ksi (MPa)	0.2%YS, ksi (MPa)	El, %	RA, %	CVN, ft-lb (J)
33	216 (1,489)	155 (1,069)	20	20	48 (65)
40	203 (1,400)	150 (1,034)	—	24	65 (88)
50	226 (1,558)	128 (883)	41	51	50 (68)
60	213 (1,469)	109 (752)	60	67	144 (196)
AISI 304	215 (1,482)	47 (324)	—	—	110 (150)

(a) UTS—ultimate tensile strength; YS—yield strength; El—elongation in 2 in. (50.8 mm); RA—reduction in area; CVN—Charpy V-notch.

Table 4—Mechanical Properties of Alloys 33, 40, 50 and 60 at 1000°F (538°C)

Alloy	UTS, ksi (MPa)	0.2%YS, ksi (MPa)	EL, %	RA, %
33	74 (510)	32 (221)	47	76
40	71 (490)	30 (207)	35	—
50	89 (614)	48 (331)	36	62
60	74 (510)	28 (193)	51	73
AISI 304	56 (386)	22 (152)	44	34

(a) UTS—ultimate tensile strength; YS—yield strength; El—elongation in 2 in. (50.8 mm); RA—reduction in area; CVN—Charpy V-notch.

Table 5—Effect of Cold Work on Alloys 33, 40, 50 and 60[a]

	60% reduction				
Alloy	UTS, ksi (MPa)	0.2%YS, ksi (MPa)	El, %	Hardness	Magnetic permeability
33	222 (1,531)	199 (1,372)	5	Rc45	1.001
40	202 (1,393)	182 (1,255)	6	Rc40	1.02
50	234 (1,613)	216 (1,489)	9	—	1.004
60	240 (1,655)	195 (1,344)	12	Rc43	1.05
AISI 304	187 (1,289)	174 (1,200)	5	Rc38	≈ 4

(a) UTS—ultimate tensile strength; YS—yield strength; El—elongation in 2 in. (50.8 mm); RA—reduction in area; CVN—Charpy V-notch.

Table 6—Wear and Galling Properties of Alloys 33, 40, 50 and 60

Alloy	Metal to particle wear[a] (lower index no. shows less wear)	Metal to metal wear,[b] mg loss/ 1000 cycles	Metal to Metal galling[c] occurs at load of indicated ksi (MPa)
33	.76	7.39	30 (207)
40	—	8.94	8 (55)
50	1.04	9.95	2 (14)
60	.76	2.79	50+ (345+)
AISI 304	1.0	12.77	2 (14)

(a) Abrasion with ceramic grit; weight loss converted to index numbers.
(b) Rotating crossed cylinders, matching materials unlubricated.
(c) Tests made with matching materials under increasing load until galling occurs.

the effect of increasing both ultimate tensile strengths and yield strengths. The higher ultimate tensile strength of Type 304 at extremely low temperatures is related to the transformation from the room temperature austenite to martensite. Note that the yield strength for Type 304 is not significantly increased.

Work Hardening

The work hardening phenomena associated with austenitic stainless steels is that of austenite transformation to martensite (a hard magnetic phase). The degree of transformation with any given amount of cold work is related to the inherent austenite stability of the alloy and the temperature at which the deformation takes place.

A very interesting phenomena associated with nitrogen strengthened alloys is that two kinds of hardening may take place. One hardening mechanism occurs with the normal transformation of austenite to martensite, and the second hardening results from the formation of epsilon phase in the cold work austenite.

All four stainless steels (i.e., alloys 33, 40, 50 and 60) considered here are very stable and do not transform to martensite on cold deformation. However, they still work harden as shown in Table 5, most probably by the formation of epsilon phase. The work hardening rate appears to be about the same as is experienced with Type 304, an alloy that hardens principally by austenite transformation to martensite. Compared to Type 304, one big difference is that the four alloys can be mechanically cold formed into components and retain their non-magnetic property normally associated with all of the austenitic stainless steels when in the annealed condition.

Wear and Galling

In looking at wear and galling characteristics, three types of wear are often considered:

1. Particle to metal wear such as in handling ores.
2. Metal to metal wear such as in gears.
3. Metal to metal galling such as in bolting.

In the first type of wear, alloys that tend to work harden on deformation wear well under the peening action of rock and ore particles. In the second and third wear applications, alloys that tend to work harden and exhibit a surface phenomena or have a high hardness and exhibit a surface phenomena will resist wear and galling under sliding loads.

The wear test data in Table 6 shows how the four stainless steel alloys perform in these areas.

Table 7—Corrosion Resistance of Alloys 33, 40, 50 and 60—Laboratory Test Media

Alloy	65% boiling nitric IPM ASTM A262-C	Boiling 42% $MgCl_2$ ASTM G58	10%$FeCl_3$ at R.T. 50 h, g/cm^2 ASTM G-48	Salt spray ASTM B117
33	0.0018	No. cracks 264 h	0.006	No rust 240 h
40	0.0012	Failed 24 h	–	No rust 720 h
50	0.0006	Failed 24 h	< 0.0002	No rust 500 h
60	0.0050	L. surf. cracks 264 h	0.0006	Some rust 120 h
AISI 304	0.0012	Failed 24 h	0.0101	Some rust 120 h

Table 8—Effect of Nitrogen on Ferrite in Autogenous Fusion Welds

Alloy	%N	FN Measured WRC Procedure	FN from the Schaeffler diagram calculated using a 0.87 blank for manganese
33	0.31	1	0 (−6)[a]
40	0.30	3	0 (−3)[a]
50	0.27	2	0 (−5)[a]
60	0.14	7	9
AISI 304	0.04	4	4

(a) A negative ferrite number indicates the relative location of a particular alloy composition in the austenite field side of the 0% ferrite line on the Schaeffler diagram.

Corrosion Resistance

The corrosion resistance of N_2 strengthened stainless steel alloys 33, 40, 50 and 60 is quite good overall, being generally equivalent to Type 304, with exceptional properties in some specific areas. For example, alloy 33, having only 3.5% Ni, exhibits a resistance to transgranular stress cracking in hot aqueous chloride containing media much better than that of Type 304. Alloy 50 exhibits exceptional resistance to pitting. Resistance to rusting in marine atmospheres for the three 0.30% nitrogen-containing alloys (33, 40 and 50) is well above that of Type 304. A summary of corrosion data relating to specific test media is given in Table 7.

Weldability

Manganese Effect

In early weld evaluations, fusion welds in base metals were made with no filler metal added. The results with alloy 40, which was the first development of the four alloys discussed here, showed the fused area to have a structure of about 3% delta ferrite in a matrix of austenite. This was fully unexpected because the Schaeffler diagram (Ref. 1) predicted a value of 0 ferrite (−3).* In fact, the DeLong diagram (Ref. 2) which allows for nitrogen also showed a value of 0 ferrite (−10).

In making comparisons with the standard stainless steels like Type 304, it was

See Table 8 for negative ferrite numbers.

Table 9—Measured FN's Compared to Calculated FN's for Alloys 33, 40, 50 and 60[a]

ID	Type	Weld process	C	Mn	Si	Cr	Ni	Mo	N	V	Cb	Meas. WRC	FN calc Mn adj	FN calc Mn + N adj
A	60	GTA	.076	8.5	4.2	17.4	8.4	–	.13	–	–	7	9	–
B	60W	SMA	.058	7.7	3.4	18.5	9.4	–	.14	–	–	4	7	–
A	35W	SMA	.070	11.2	.36	18.3	4.8	–	.16	–	–	6	5	–
B	35W	SMA	.059	10.8	.33	18.7	4.8	–	.17	–	–	4	6	–
L	35W	SMA	.060	13.5	.10	18.2	5.2	–	.17	–	–	4	3	–
D	35W	SMA	.068	13.4	.10	19.2	5.1	–	.18	–	–	5	7	–
F	35W	GMA	.042	11.7	.46	18.3	4.2	–	.19	–	–	6	8	–
E	35W	GMA	.042	11.8	.47	18.5	4.2	–	.20	–	–	7	7	–
A	50W	SMA	.046	6.1	.41	20.9	10.1	1.8	.21	.23	–	5	3	7
B	50W	SMA	.046	6.2	.32	21.1	10.3	1.8	.21	.23	–	7	3	7
S	50W	SMA	.033	6.5	.26	21.6	10.3	1.9	.21	.25	–	8	6	9
E	50W	SMA	.047	6.1	.41	21.9	10.5	2.0	.22	.24	–	9	5	8
N	50	GTA	.038	4.7	.55	21.0	12.5	2.2	.23	.16	.18	3	(−2)	2
F	50W	SMA	.034	6.1	.38	21.4	10.6	1.8	.24	.22	–	8	3	7
D	50W	GMA	.036	6.2	.60	21.6	10.6	1.8	.25	.23	–	7	3	7
L	50	GTA	.036	4.8	.46	21.5	12.6	2.2	.25	.15	.17	2	(−2)	2
Q	40W	SMA	.030	8.3	.42	20.3	6.8	–	.25	–	–	5	1	6
M	50	GTA	.041	5.0	.47	21.7	12.7	2.2	.26	.18	.16	5	(−3)	2
J	50	GTA	.050	5.4	.42	21.5	12.4	2.1	.27	.19	.20	1	(−3)	1
O	50	GTA	.043	4.8	.52	20.9	12.7	2.2	.28	.17	.17	0	(−6)	(−1)
K	40	GTA	.027	9.1	.64	20.3	7.1	–	.28	–	–	3	(−2)	5
H	40	GTA	.026	8.8	.72	20.1	7.0	–	.29	–	–	4	(−2)	6
E	40	GTA	.033	8.9	.64	20.3	7.3	–	.30	–	–	2	(−3)	3
F	40	GTA	.020	8.9	.68	20.2	7.2	–	.31	–	–	2	(−3)	4
N	40	GTA	.017	8.9	.73	20.1	7.2	–	.32	–	–	3	(−3)	3
D	40	GTA	.022	9.2	.62	20.2	7.1	–	.33	–	–	2	(−4)	3
O	33	GTA	.057	12.8	.42	17.5	3.7	–	.33	–	–	1	(−7)	1

(a) The nitrogen effect determined from this work appeared best summarized for use with the Schaeffler diagram as follows:
1. Use 0.045 nitrogen residual for Schaeffler diagram calculations.
2. For nitrogen 0% to 0.20%, use (%N − 0.045) × 30 as a plus value in the nickel equivalent.
3. For nitrogen 0.21% to 0.25%, use (%N − 0.045) × 22 as a plus value in the nickel equivalent.
4. For nitrogen 0.26% to 0.35%, use (%N − 0.045) × 20 as a plus value in the nickel equivalent.

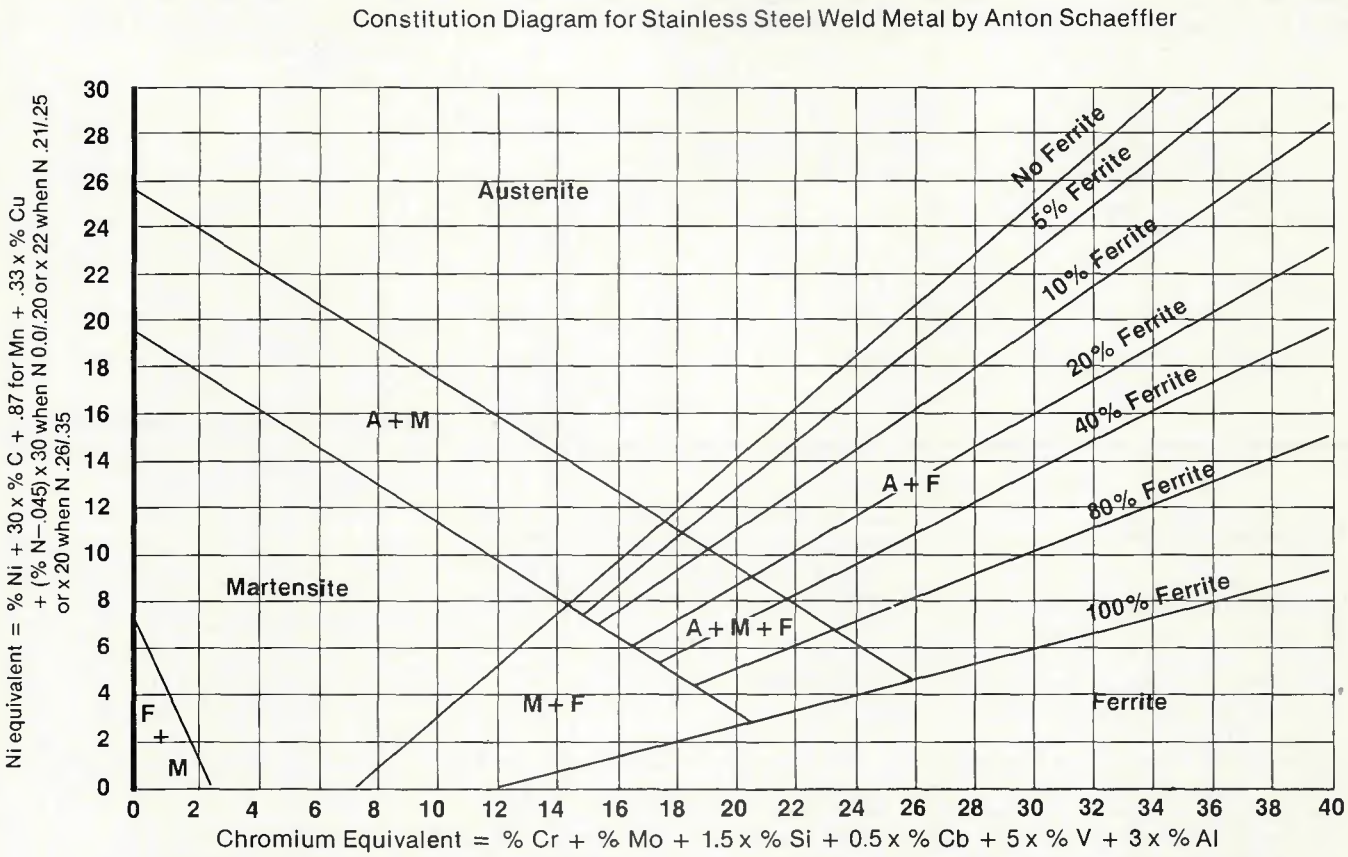

For average size stainless steel alloy welds (5/32" ϕ electrode — SMA process) including the Mn N modifications (Mn up to 15% — N up to .35%) the % of Ferrite (up to ≈ 30%) in a matrix of Austenite or Austenite + Martensite or Martensite can be predicted within ≈ 4%. The % of Ferrite is considered equivalent to the WRC — FN (Ferrite Number). The faster freezing rate of a smaller than average size weld gives lower Ferrite contents than predicted by the diagram and conversely the slower freezing rate of a larger than average size weld results in higher ferrite contents. With Mn contents greater than 2.5% and Copper contents greater than .5% the Austenite resistance to Martensite transformation increases expanding the stable Austenite region to a more broad area than shown in the above diagram.

Fig. 1—Schaeffler constitution diagram for stainless steel weld metal modified for manganese with nitrogen, vanadium, copper and aluminum added (adapted by R. Harry Espy)

determined that the *manganese factor* for both the Schaeffler and DeLong diagrams did not reflect the true effect of that element. In fact, it appeared that the manganese had little effect on weld structures as an austenite former.

A similar observation on this effect of manganese was reported by Guiraldeng (Ref. 3) in 1967 and by Hull (Ref. 4) in 1973. To use the Schaeffler and DeLong diagrams in a realistic way, the nickel equivalent was changed to read:

$30 \times \%C + .87 + \%Ni + 30 (\%N - .045)$ for Schaeffler, and $30 \times \%C + .87 + \%Ni + 30\%N$ for DeLong.

The Schaeffler diagram modified for manganese and nitrogen was selected for all future work, because it encompassed the total stainless steel range. The constant number of 0.87 for manganese regardless of actual content was based on the average manganese content of the weld deposits used in developing the Schaeffler diagram which was 1.75% Mn × 0.5 equaling 0.87. The constant of 0.045 used with nitrogen was based on the residual nitrogen content of these same welds being reported as an average of 0.045.

Nitrogen Effect

Applying the modified nickel equivalent to the four alloys showed that calculated and measured values deviated in what appeared to be a function of *nitrogen content*. Shown in Table 8 are FNs (Ferrite Numbers) typical of those obtained with autogenous welds in the four alloys covered here. From the data, it appeared that the effect of nitrogen as an austenite former at levels of about 0.26% and above was somewhat different than the 30 multiplication factor usually employed as a nickel equivalent.

In developing filler metals for joining these alloys, the first objective was to balance the composition to produce weld structures of ferrite in a matrix of austenite. Matching filler metals having a nitrogen content near that of the base metal were often found to deposit welds that were porous and much stronger than the base metal to be welded. So, as a rule, nitrogen contents were lowered and the alloys rebalanced to give the desired structure of ferrite in a matrix of austenite. Rebalancing was based on the Schaeffler diagram with the nickel equivalent modified using a manganese blank of 0.87.

In the course of filler metal development work, compositions having a wide range of nitrogen contents were examined. The reduced effect of nitrogen as an austenite former at high levels was evident here in a manner similar to that seen with the autogenous welds. A number of compositions typical of those studied are shown in Table 9 along with results from several autogenous welds.

Figure 1 is the Schaeffler diagram modified by the author for the elements manganese, nitrogen, vanadium, copper and aluminum. The elements vanadium, copper and aluminum have been added to the diagram from other work. Figure 2 is the same diagram with points showing the location of compositions typical for autogenous welds in alloys 33, 40, 50 and 60. The filler metals for each alloy are also included to indicate the ferrite-austenite relationship.

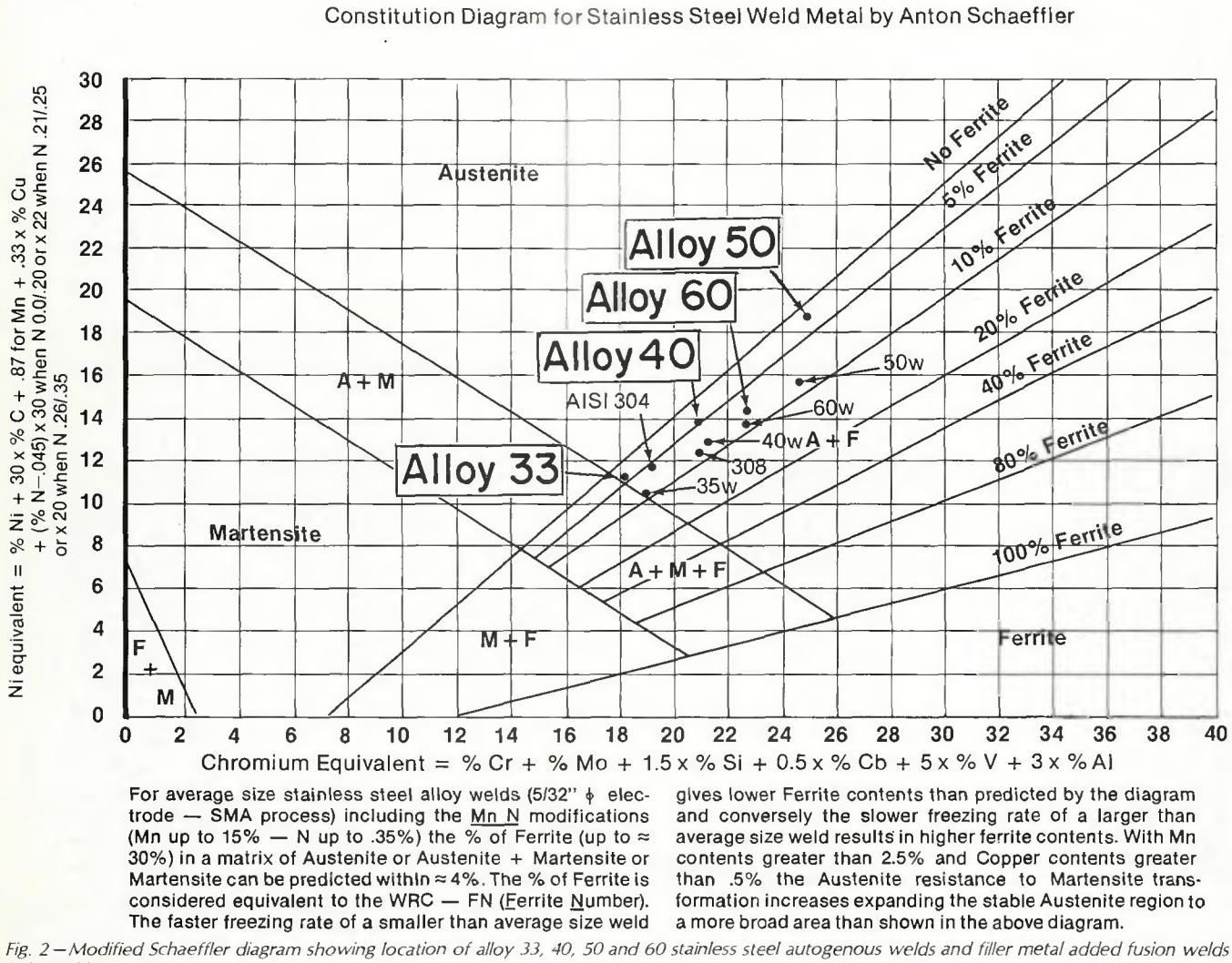

For average size stainless steel alloy welds (5/32" ϕ electrode — SMA process) including the Mn N modifications (Mn up to 15% — N up to .35%) the % of Ferrite (up to ≈ 30%) in a matrix of Austenite or Austenite + Martensite or Martensite can be predicted within ≈ 4%. The % of Ferrite is considered equivalent to the WRC — FN (Ferrite Number). The faster freezing rate of a smaller than average size weld gives lower Ferrite contents than predicted by the diagram and conversely the slower freezing rate of a larger than average size weld results in higher ferrite contents. With Mn contents greater than 2.5% and Copper contents greater than .5% the Austenite resistance to Martensite transformation increases expanding the stable Austenite region to a more broad area than shown in the above diagram.

Fig. 2—Modified Schaeffler diagram showing location of alloy 33, 40, 50 and 60 stainless steel autogenous welds and filler metal added fusion welds (adapted by R. Harry Espy)

Weld Metal Properties

All weld deposits made using the AWS procedure (Ref. 5) for each of the four filler metals showed the deposits to be strong, ductile, tough and free of defects. All deposits contained a small amount of ferrite in a matrix of austenite. In all cases, weld deposit strengths were equal to or better than those of the unwelded base metals.

The all-weld-metal properties and compositions for each of the filler metals are shown in Table 10.

Weld Structures

A typical autogenous weld structure for alloy 33 is shown in Fig. 3. The structure is one of about 3% delta ferrite in a matrix of austenite. Note the delta ferrite formation in the high temperature area of the unfused base metal. The formation of ferrite in this base metal area is highly desirable in avoiding underbead cracking.

A typical weld structure for an all-weld-alloy 50 multipass deposit is shown in Fig. 4. The structure is one of about 6% delta ferrite in a matrix of austenite. Here again, the presence of ferrite in the underbead area is important in avoiding cracking in the heat affected areas of multipass welds. Figure 5 shows a fractured tensile specimen from an all-weld deposit of alloy 50W stainless steel and illustrates the good ductility and strength typical of N_2 strengthened weld metal.

Weld Joint Properties

The properties of weld joints in several thicknesses of material made using conventional weld processes are shown in Tables 11, 12, and 13 for stainless steel alloys 33, 40, and 50, respectively. Shown for comparison are properties of unwelded base materials in both sheet and plate materials.

The data show that weld joints have mechanical properties equivalent to those of the unwelded base materials.

Corrosion of Weldments

The corrosion resistance of weld areas in austenitic stainless steels is often considered on the basis of carbide precipitation when sensitized by the heat of welding. Work reported by the Welding Institute (Ref. 6) indicated that nitrogen, like molybdenum, retards the diffusion of carbon to grain boundaries. In effect, longer times are required for damaging carbides to form. The result is that, for welding when nitrogen is at 0.30%, carbon levels up to about 0.06% may be present before indications of damaging carbides are noted.

Even with carbon at 0.10% the formation of carbides in welding is significantly less than in a 0.10% carbon austenitic stainless having only residual nitrogen content. Figure 6 shows that alloy 33 having a carbon level of 0.05% can be sensitize heat treated to simulate welding for a period of about 20 minutes (min) before damaging carbides begin to form. At 40 min, the formation of damaging carbides as measured by corrosion was only a small percentage of that experienced with Type 304 stainless steel. Even tests that retarded cooling rate from the

Table 10—Typical Composition and Properties[a] of Alloy 33, 35, 40, 50 and 60 Weld Deposits

Alloy	Composition, %									FN of weld deposit	UTS, ksi	0.2YS, ksi	El, %	RA, %	CVN, ft/lb
	C	Mn	Si	Cr	Ni	Mo	N	V	Cb						
33	0.05	12	0.40	17.5	3.5	–	0.31	–	–	2	–	–	–	–	–
35W	0.05	12	0.40	18	5	–	0.15	–	–	7	106	83	34	52	62
40	0.03	9	0.60	20.5	6.7	–	0.30	–	–	4	–	–	–	–	–
40W	0.03	9	0.40	20.5	6.5	–	0.25	–	–	6	107	86	33	47	47
50	0.04	5	0.40	21.25	12.25	2.25	0.27	0.14	0.14	2	–	–	–	–	–
50W	0.03	6	0.40	21.0	10.0	1.7	0.22	0.20	–	7	105	83	36	51	52
60	0.07	8	4.00	16.5	8.25	–	0.14	–	–	6	–	–	–	–	–
60W	0.07	8	4.00	16.5	8.25	–	0.12	–	–	7	109	78	19	18	41
AISI 304	0.06	1.4	0.50	18.25	9.0	–	0.04	–	–	5	–	–	–	–	–
AWS 308	0.04	2	0.50	20.25	10.25	–	0.045	–	–	7	89	68	37	51	53

(a) UTS – ultimate tensile strength; YS – yield strength; El – elongation in 2 in. (50.8 mm); RA – reduction in area; CVN – Charpy V-notch.

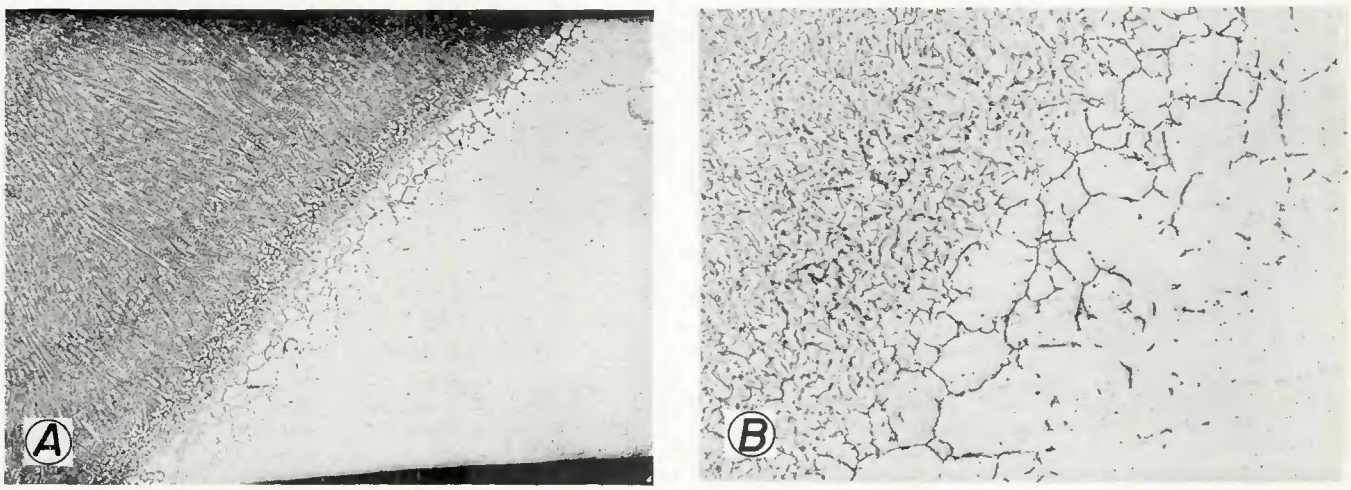

Fig. 3 – Weld-base metal interface of autogenous fusion weld in alloy 33 stainless steel. Structure – ferrite in a matrix of austenite; etchant – ammonium persulfate. A – X100; B – X400 (reduced 30% on reproduction)

solution anneal (1950°F, i.e., 1066°C) by shelving at 1250°F or 677°C (see Fig. 7) showed only a small increase in corrosion when exposed for times up to 2 hours (h).

These results indicate that cooling rates of annealed areas from weld temperatures are not as critical in the nitrogen strengthened alloys. In addition, this work shows that 33, 40, 50 and 60 alloys may not require rapid cooling (water quench of heavy sections) from solution anneal heat treatments during manufacture and in fabrication. Air cooling appears to give satisfactory results.

The general thinking concerning carbide precipitation with the N_2 strengthened stainless steels may be applied to alloys 33, 40 and 50 but is not applicable to alloy 60. While alloy 60, like other nitrogen bearing alloys, does not form damaging carbides rapidly when heated to sensitizing temperatures, it is sensitive to grain boundary precipitates if not rapidly cooled from the solution annealing temperature.

Applications

Typical weldments in the four alloys are shown in Figures 8 – 11. Figure 8 is a photograph of conduit for electrical cable where non-magnetic austenitic stainless steels have been used to reduce eddy current loss. When stainless steels like Type 304 are cold formed in the field for installation, they become magnetic because of martensite formation and require post form annealing to regain nonmagnetic characteristics. Alloy 33 retains its non-magnetic characteristics even when severely cold formed. The low magnetism caused by ferrite in the weld metal is not sufficient to create overheating in these relatively small weld areas during service.

Fig. 4 – Weld pass interface area in an all-weld multipass deposit of alloy 50W stainless steel. Structure – ferrite in a matrix of austenite; etchant – NaOH. X500 (reduced 38% on reproduction)

Figure 9 illustrates a component of an aerospace fire extinguisher system used in a commercial jet airliner. The component consists of alloy 40 machined fittings and formed sheet stock joined into a finished component by welding.

Figure 10 is a photograph of a pressure vessel made of alloy 50 formed plate and fabricated by welding. The vessel is used in a highly corrosive environment for containing nuclear materials.

Figure 11 depicts a Type 410 stainless steel valve showing both gate and seal areas surfaced with alloy 60W filler metal and machined flush.

Discussion

The manganese-nitrogen modified austenitic stainless steels considered in this

work possess interesting and useful properties. Compared to the conventional austenitic stainless steels, alloys 33 and 60 show significant improvement in resistance to transgranular stress corrosion. Alloys 33 and 60 possess striking wear and galling resistance properties. All four alloys have high strengths with good ductility and toughness from cryogenic to elevated temperatures.

The weldability of these alloys is good, being comparable to the conventional austenitic stainless steels like Types 304L and 316L. There is, however, one significant area of difference, that being porosity from nitrogen associated with high speed tube welding or welding under reduced pressures like electron-beam in vacuum. The entrapped gas or porosity can, in both cases, be eliminated by reducing weld travel speeds in tube welding and by using two-pass techniques in electron-beam welding. In both cases, additional time is needed for outgassing. The tendency toward a more than normal outgassing is directly related to nitrogen content. When filler metal is added during the welding of alloys 33, 40, 50 and 60, the matching fillers metal have nitrogen contents lower than the base materials for the specific purpose of controlling porosity.

In reports by Bennett (Ref. 7) and Brooks (Ref. 8), it was indicated that unusual problems of penetration and cracking in gas tungsten arc and electron-beam welding are to be expected. Increased levels of manganese (an integral part of the four alloys) do tend to create a less fluid weld surface condition when low resistance weld shield gases like argon are employed. Because of this lower fluidity condition, the more resistant shielding gases like argon +5% hydrogen, helium, or helium +5% hydrogen are used, resulting in a very normal weld width and penetration.

The weld cracking situation is no different than that encountered with Type 304L stainless steel. In fact, all four alloys, like Type 304L for autogenous weld applications, are manufactured to give weld structures resistant to hot cracking. The selection and testing of compositions not intended for autogenous welding, as done by Brooks (Ref. 8), would obviously result in cracking much the same as happens with Type 304L stainless steel that does not possess the proper composition designed to resist weld cracking.

Sound and defect-free welds in alloys 33, 40, 50 and 60 having corrosion and mechanical properties equivalent to the unwelded base metals are readily made by both autogenous and filler metal added welding procedures.

Conclusion

Alloys 33, 40, 50 and 60 have very

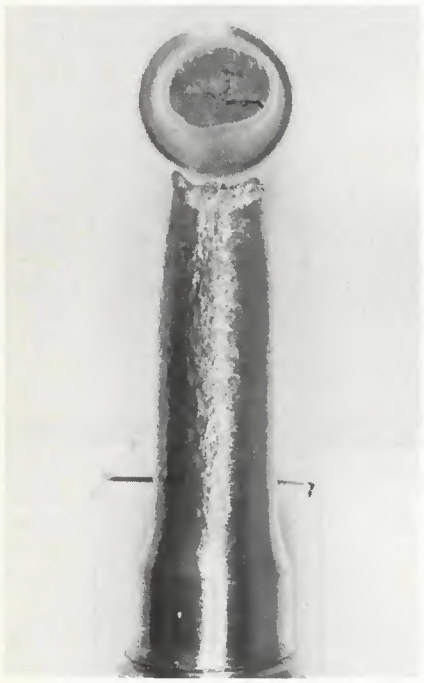

Fig. 5—Fractured tensile specimen machined from 1 in. (25.4 mm) thick all-weld deposit of alloy 50W stainless steel. Ultimate tensile strength—105 ksi (724 MPa); 0.2% yield strength—83 ksi (572 MPa); elongation in 2 in.—36%; reduction in area—51%

Table 11—Mechanical Properties[a] of As-Welded Joints in Alloy 33 Made with Alloy 35W Filler Metal

Joint thickness, in.	Welding process[b]	UTS ksi (MPa)	0.2YS, ksi (MPa)	El, %	Failed in[c]
0.062	Unwelded sheet	115 (793)	68 (469)	61	—
0.062	GTA	114 (786)	68 (469)	40	WM/BM
0.250	SMA	104 (717)	63 (434)	24	WM
0.750	SMA	106 (731)	67 (462)	46	WM
0.750	Unwelded plate	106 (731)	67 (462)	54	—

(a) UTS—ultimate tensile strength; YS—yield strength; El—elongation in 2 in. (50.8 mm); CVN—Charpy V-notch.
(b) GTA—gas tungsten arc; SMA—shielded metal arc.
(c) WM—weld metal; BM—base metal.

Table 12—Mechanical Properties[a] of As-Welded Joints in Alloy 40 Made with Alloy 40W Filler Metal

Joint thickness, in.	Welding process[b]	UTS, ksi (MPa)	0.2YS ksi (MPa)	El, %	Failed in[c]
0.062	Unwelded sheet	112 (772)	68 (469)	44	—
0.062	GTA	109 (752)	68 (469)	22	WM
0.750	SMA	107 (738)	67 (462)	32	WM
2.0	SMA	101 (696)	63 (434)	26	WM
4.0	Unwelded plate	103 (710)	58 (400)	50	—

(a) UTS—ultimate tensile strength; YS—yield strength; El—elongation in 2 in. (50.8 mm); RA—reduction in area; CVN—Charpy V-notch.
(b) GTA—gas tungsten arc; SMA—shielded metal arc.
(c) WM—weld metal.

Table 13—Mechanical Properties[a] of As-Welded Joints in Alloy 50 Made with Alloy 50W Filler Metal

Joint thickness, in.	Welding process[b]	UTS, ksi (MPa)	0.2YS ksi (MPa)	El, %	Failed in[c]
0.062	Unwelded sheet	111 (765)	62 (427)	44	—
0.062	GTA	98 (676)	60 (414)	15	WM
0.250	SMA	105 (724)	63 (434)	21	WM
1.250	GMA	112 (772)	77 (531)	21	WM
1.00	Unwelded plate	120 (827)	65 (448)	45	—

(a) UTS—ultimate tensile strength; YS—yield strength; El—elongation in 2 in. (50.8 mm).
(b) GTA—gas tungsten arc; SMA—shielded metal arc; GMA—gas metal arc.
(c) WM—welded metal.

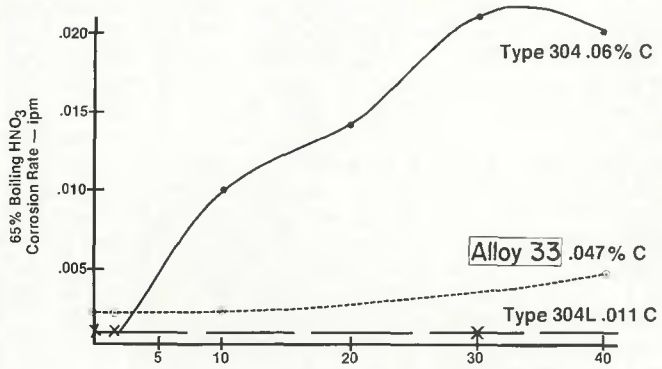

Fig. 6 — Effect of nitrogen in alloy 33 in reducing damaging grain boundary precipitates as measured by corrosion susceptibility using ASTM A262-C after a sensitize heat treatment

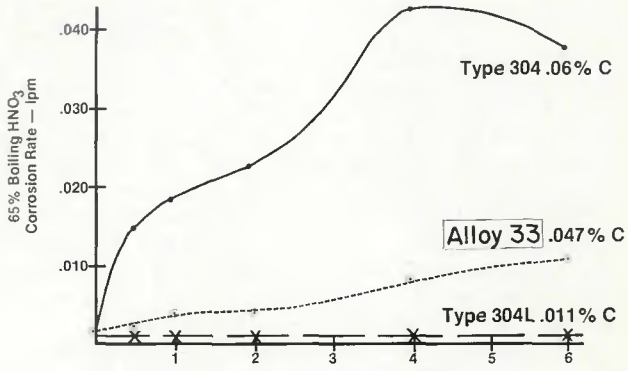

Fig. 7 — Effect of nitrogen in alloy 33 in reducing damaging grain boundary precipitates as measured by corrosion susceptibility using ASTM A262-C when rate of cool from solution anneal temperature is retarded

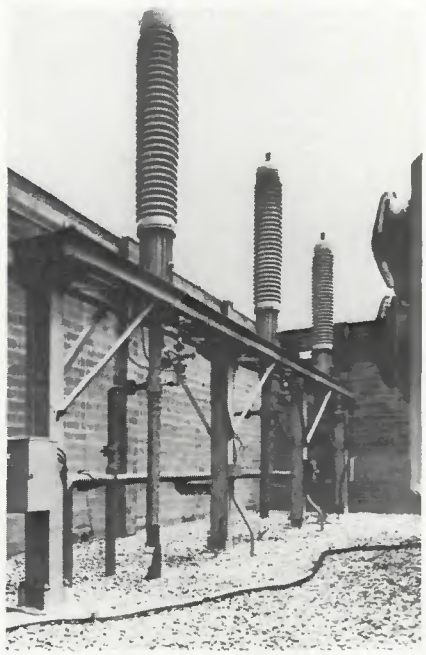

Fig. 8 — Welded alloy 33 stainless steel pipe for undergound electrical conduit installations. Termination of line where the phases are separated is shown

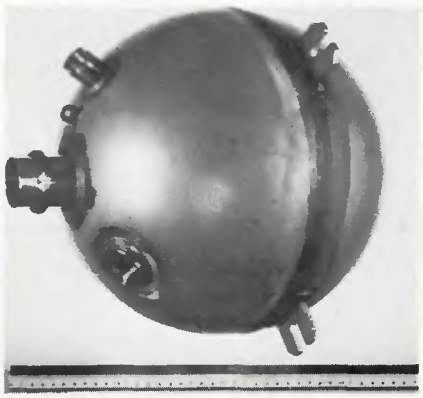

Fig. 9 — Welded alloy 40 stainless steel vessel used in aerospace fire extinguisher systems

Fig. 10 — Welded alloy 50 stainless steel pressure vessel for highly corrosive nuclear application

Fig. 11 — Type 410 stainless steel valve gate and seal areas after being surfaced with alloy 60W for wear and galling resistance

interesting mechanical, corrosion and physical properties which are useful in numerous applications. High strengths over a wide range of temperatures, improved resistance to pitting and stress corrosion and retention of non-magnetic characteristics have been useful in weight reduction, better life in severe corrosive media and lower cost in fabrication.

Suitable filler metals capable of producing sound welds having properties matching those of the unwelded base metals have been developed and are available.

The Schaeffler diagram commonly used for predicting stainless steel weld structures was modified by changing manganese and nitrogen factors for use with these manganese-nitrogen modified stainless steels. The weldability and performance of weldments in these steels (i.e., alloys 33, 40, 50 and 60) are rated as very good.

References

1. Schaeffler, Anton. 1949 (Nov.). Constitution diagram for stainless steel weld metal. *Metal Progress,* data sheet, p. 680 B.

2. DeLong, W. T.; Ostrom, G. A.; and Szumachowski, E. R. 1956. Measure and calculation of ferrite in stainless steel weld metal. *Welding Journal* 35(11): 521-s to 528-s.

3. Guiraldeng, P. 1967 (Nov. P). *Memorandum science review metal* 64.

4. Hull, F. C. 1973. Delta ferrite and martensite formation in stainless steels. *Welding Journal* 52(5): 193-s to 203-s.

5. American Welding Society. 1978. *Specification for corrosion resisting chromium and chromium-nickel steel covered welding electrodes (AWS 5.4-78).* Miami.

6. Gooch, T. G. 1969 (Dec.). The corrosion behavior of welded nitrogen bearing austenitic stainless steels. *Metal Construction and British Welding Journal:* 569-574.

7. Bennett, W. S., and Mills, G. S. 1974. Weldability studies on high manganese stainless steel. *Welding Journal* 53 (12): 548-s to 553-s.

8. Brooks, J. A. 1975. Weldability of high nitrogen high manganese austenitic stainless steel. *Welding Journal* 54(6): 189-s to 195-s.